Phosphine-Stabilized Ruthenium Nanoparticles: The Effect of the Nature of the Ligand in Catalysis

David González-Gálvez,[†] Pau Nolis,[‡] Karine Philippot,[§] Bruno Chaudret,[⊥] and Piet W. N. M. van Leeuwen*,[†]

[†]Institute of Chemical Research of Catalonia (ICIQ), 43007 Tarragona, Spain

[‡]Servei de Ressonància Magnètica Nuclear, Universitat Autònoma de Barcelona, 08193 Bellaterra, Spain

[§]LCC (Laboratoire de Chimie de Coordination du CNRS), CNRS, 205 route de Narbonne, F-31077 Toulouse, France and Université de Toulouse, UPS, INPT, LCC; F-31077 Toulouse, France

[⊥]Laboratoire de Physique et Chimie des Nano-Objets, Institut des Sciences Appliquées de Toulouse, 31077 Toulouse, Cédex 04, France

S *Supporting Information*

ABSTRACT: Various ligands not forming monometallic complexes were used for Ru nanoparticle stabilization, enabling the control of size, shape, and electronic properties. HRMAS NMR spectroscopy allowed us to study surface-bound molecules, evidencing ligand hydrogenation and decomposition of THF during the RuNP synthesis. Catalysis studies underscore the importance of the nature of the ligands. The RuNPs were tested in the hydrogenation of aromatics, showing very high activities (TOF > 60 000 h^{-1}, 40 bar, 393 K). A pronounced ligand effect was found, and dialkylaryl phosphine ligands gave the fastest catalyst.


KEYWORDS: *ruthenium nanoparticles, ligand effect, HRMAS NMR, surface-bound molecules characterization, hydrogenation of aromatics*
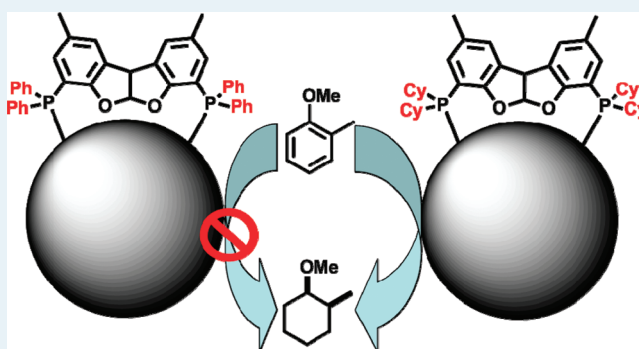
During the past decade, metal nanoparticles (MNPs)[1] have been studied extensively as part of the large effort devoted to the development of nanosized materials in all areas of science and technology, including heterogeneous catalysis. In recent years, ruthenium nanoparticles have emerged as one of the most active catalysts for complete hydrogenation of aromatics, providing high activities under mild conditions.[2−4] In the presence of RuNPs, the important selective transformation of benzene into cyclohexene has also been reported.[5−7]

Nowadays, the development of new stabilizers enabling modification and control of the properties of RuNPs (size, surface structure, electronic properties) remains a challenge. In these studies, one generally aims at colloidal solutions of highly dispersed NPs that allow the study of these materials, without the interaction of supports. In our group, roof-shaped diphosphines **1−3** and monophosphine **4** (Chart 1) were designed for making polymetallic complexes that were used in catalysis.[8,9] These phosphines are expected to form strong bonds to a metal cluster via the phosphorus atoms, and in addition, they show a weak π−π interaction between the aromatic backbone and the ruthenium atoms, thus providing a dynamic surface coverage. Characterization of the ligands coordinated on the cluster surface is important to obtain a

Chart 1. Ligands Used As RuNPs Stabilizers
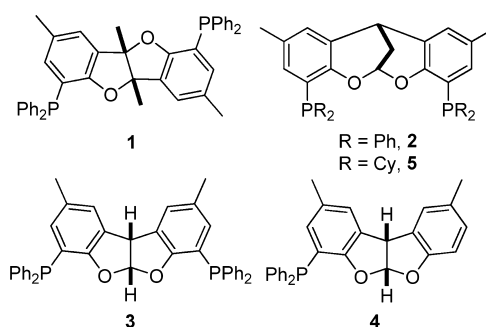
better understanding of the properties, in particular since they can be significantly transformed under the conditions of the synthesis of the MNPs. High resolution-magic angle spinning (HRMAS) is a powerful NMR accessory that allows one to obtain good quality spectra of samples having a high degree of heterogeneity. Recently, HRMAS NMR spectroscopy was introduced as a technique for studying NP-bound mole-

cules;[10−13] it reduces the line-broadening usually obtained when liquid-state NMR experiments are performed on such systems.

Notably, HRMAS spectroscopy affords high spectral resolution because only the soluble part of the sample or the part that presents a sufficient degree of mobility is detected, whereas in solid-state NMR, the whole rigid system is analyzed, which possesses a high chemical shift anisotropy and strong dipolar interactions, both of which contribute to appreciable broadening of the NMR signals.

Eight different mono- or diphosphine stabilized ruthenium(0) NPs (Ru-ligand[eq], eq = ligand/Ru ratio) were prepared by decomposition of a THF solution of the organometallic precursor [Ru(COD)(COT)] in the presence of 0.1 or 0.2 eq of the corresponding phosphine (higher ligand ratios produced mainly molecular compounds, and lower ratios gave unstable materials) under dihydrogen (3 bar), in a way similar to that described previously (room temperature, 18 h).[14,15] Small and soluble RuNPs (1.1−2.1 nm; TEM images in Figure 1) were provided, the size of which could be controlled
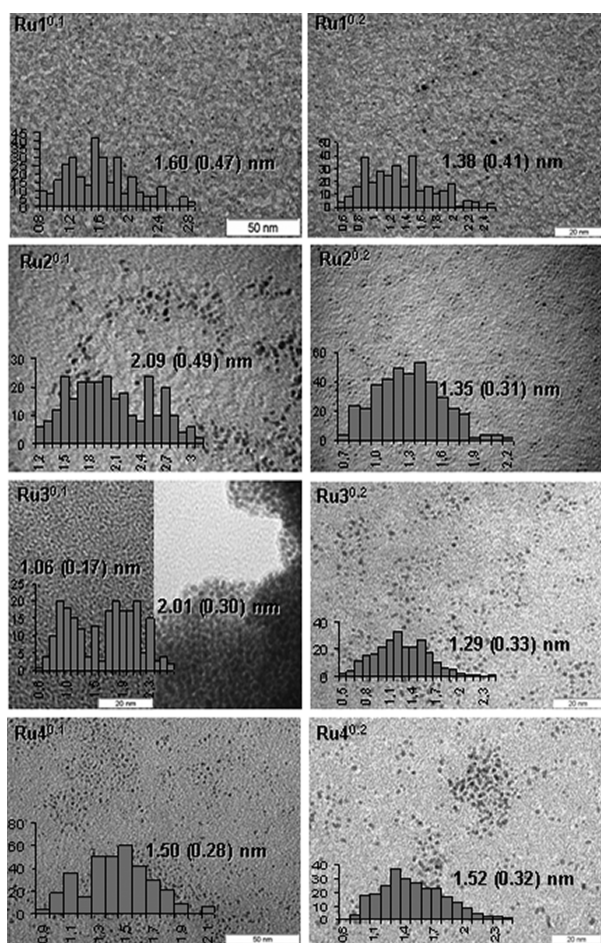

Figure 1. TEM images of RuNPs and their size distribution.

by the phosphine, the number of equivalents used, or both. For monophosphine **4**, the size is not influenced by the amount of phosphine, which may be due to equilibration between the nanoparticles.

TEM images also show that the diphosphines with both phosphines on the same side of the backbone (syn), **2** and **3**, and monophosphine **4** give better dispersed RuNPs than the

diphosphine with one phosphine on each side (anti), **1**, which gives aggregated RuNPs. The latter could be explained by a close interaction between the organic backbone and the ruthenium nanocluster in Ru1, due to the strong Ru−P bonds forcing the backbone to be oriented onto the metal surface in the case of the anti diphosphine, whereas in syn diphosphines, the organic backbone can interact more strongly with the solvent, thus providing better dispersion. Another explanation could be that the anti diphosphine could act as a linker between two particles, thus causing aggregation. Independent of the dispersion, all MNPs are quite soluble in several solvents, protic (MeOH, EtOH, 2-PrOH) as well as aprotic solvents (THF, toluene).

HRMAS NMR spectroscopy was used for the characterization of the molecules bound at the cluster surface. ^{31}P-HRMAS NMR spectra were recorded spinning the samples at 4 kHz (with no significant improvement at higher spinning rates) and a 5 s relaxation time between the experimental scans. Very poor spectra were obtained when shorter relaxation recovery delay times were used due to signal saturation (see Supporting Information (SI) Figure S1). In Figure 2, the huge difference in
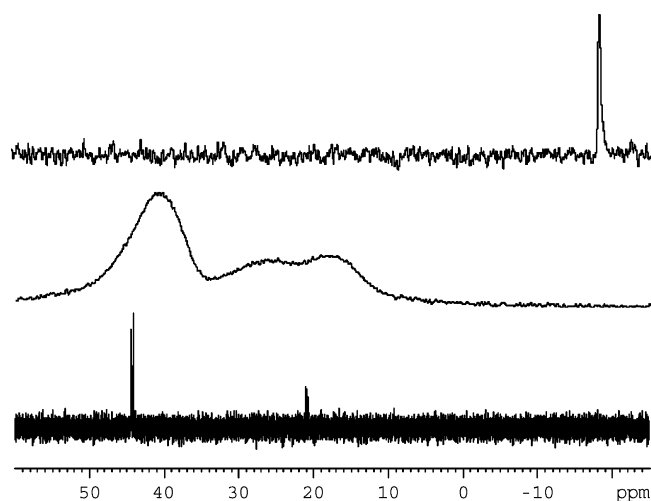

Figure 2. ^{31}P NMR spectrum of **3** (top), ^{31}P-CPMAS (middle) and HRMAS NMR (bottom) spectra of Ru3[0.2].

information obtained between solid-state ^{31}P CPMAS and HRMAS NMR spectra can be observed; HRMAS has very good resolution and, therefore, is a very useful technique for complex, soluble nanomaterials.

In the ^{31}P HRMAS NMR spectra of the RuNPs samples (Figure 3), we can observe signals in the 20 ppm area, which correspond to triarylphosphines coordinated to the ruthenium cluster ($Ar_3P−Ru$), signals between 40 and 45 ppm that correspond to dialkylarylphosphines ($Alk_2ArP−Ru$), and signals between 45 and 50 ppm that correspond to trialkylphosphines ($Alk_3P−Ru$). In all cases, the signals correspond to ligated compounds and not to free phosphines, as confirmed by comparison with free ligand spectra (Figure 2) and by 2D-DOSY experiments (see SI, Figure S2). The addition of H_2O_2 to any of the samples led to the appearance of new signals corresponding to phosphine oxide in the NMR spectra. This proves that the signals in the NMR spectra of the RuNPs correspond well to coordinated phosphines and not to oxidized ones (see SI, Figure S3).
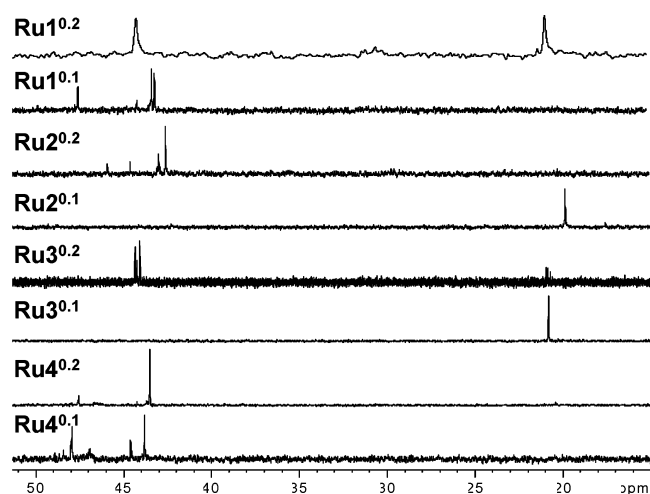
Figure 3. ^{31}P-HRMAS NMR spectra.

^{1}H-HRMAS NMR and ^{1}H−^{31}P HSQC HRMAS NMR experiments (see SI, Figures S5 and S6) corroborate the deductions made before and allow full characterization of the bound molecules. The spectra show that, depending on the ligand used and the equivalents added, very different materials were obtained (see Table 1). A key feature is the hydrogenation

Table 1. Comparison of the Nature of the Stabilizer, Nanocluster Size and Activity in the Hydrogenation of O-Methylanisole

	material	observed molecules	size (nm)	conversion (de[b])	TOF (h^{-1})[c]
				o-methylanisole hydrogenation	
1	Ru1$^{0.1}$	Alk$_2$ArP (+ Alk$_3$P)	1.60	100 (88)	29 (121)
2	Ru1$^{0.2}$	Alk$_2$ArP + Ar$_3$P	1.38	48 (90)	8
3	Ru2$^{0.1}$	Ar$_3$P	2.09	0 (−)	0
4	Ru2$^{0.2}$	Alk$_2$ArP	1.35	100 (87)	59 (92)
5	Ru3$^{0.1}$	Ar$_3$P	1.06/2.01	12 (89)	2
6	Ru3$^{0.2}$	Alk$_2$ArP + Ar$_3$P	1.29	67 (88)	18 (34)
7	Ru4$^{0.1}$	Alk$_2$ArP + Alk$_3$P	1.50	41 (91)	6
8	Ru4$^{0.2}$	Alk$_2$ArP	1.52	100 (87)	67 (152)
9	Ru5$^{0.1}$	Alk$_2$ArP	1.78	34[d] (88)	15[d] (221)

[a]Reaction conditions: 40 bar H$_2$, 295 K, 0.125 M in THF, 1% of total Ru. [b]Diastereomeric excess between cis and trans isomers. [c]Calculated considering the moles of H$_2$ consumed per atom of total Ru and per hour after 16 h of reaction; in brackets is the initial TOF in the kinetic study (20 min of reaction). [d]0.33% of total Ru.

of the aromatic groups of the ligands during the synthesis of the RuNPs, a feature that had been seen before in RuNPs stabilized with dppb.[16] Ru2$^{0.1}$ and Ru3$^{0.1}$ mainly retained the ligands as they were added initially (Ar$_3$P−Ru); in Ru1$^{0.1}$, Ru2$^{0.2}$, and Ru4$^{0.2}$, the diphenylphosphino groups were reduced to dicyclohexylphosphino groups (Alk$_2$ArP-Ru);[17] Ru3$^{0.2}$ and Ru1$^{0.2}$ contained a mixture of reduced and nonreduced ligands (Alk$_2$ArP−Ru and Ar$_3$P−Ru); and finally, Ru4$^{0.2}$ contained a mixture of completely and partially reduced ligands (Alk$_2$ArP−Ru and Alk$_3$P−Ru). These results could indicate that at low ligand ratio, Ru2$^{0.1}$ and Ru3$^{0.1}$, the ligands first coordinate to the apexes, where they are not hydrogenated and that the next ligand that comes in can interact with the faces and thus can be hydrogenated, as in Ru2$^{0.2}$ and Ru3$^{0.2}$. Monophosphine **4** can

be more easily hydrogenated, thanks to its flexibility. This was recently observed in RuNPs stabilized by NHCs.[18]

Most strikingly, the ^{1}H HRMAS NMR spectra do not show any sign of THF or polyTHF (see Figure 4 and SI Figure S5),
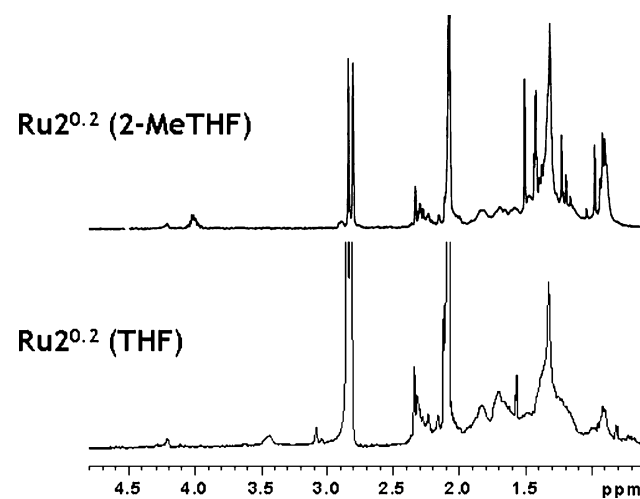

Figure 4. ^{1}H HRMAS NMR (400 MHz, acetone-d_6) spectra of Ru2$^{0.2}$ prepared in 2-MeTHF (top) and THF (bottom).

although MNPs synthesized this way are known to contain THF (30−70%).[19−21] Instead, traces of γ-butyrolactone, 2-buten-1-ol, and butanol were observed, and the major organic component present is a highly branched, high-MW alkane. A typical analysis of Ru3$^{0.2}$ showed 26.7% of Ru, 30.4% of **3** (metal/ligand = 6:1), and >40% of a polymeric hydrocarbon (see SI Table S1). This high-MW alkane could come from THF degradation, C−O and C−N bond cleavage of THF and pyrrolidine (in the cases when this is used) over MNP surfaces leading to butanol, butanamine, and even butane and water or ammonia.[22] Some of these materials were synthesized in 2-MeTHF instead of THF and analyzed by ^{1}H HRMAS NMR. In Figure 4, comparison between the same material prepared in THF or 2-MeTHF reveals some changes at high field of the spectrum. The most significant changes are new peaks around 1.5 ppm that can be assigned to hydrogen atoms at tertiary carbons of an alkane, a high ratio of the primary/secondary carbon due to the methyl group in 2-MeTHF, and a new signal around 4.0 ppm that is probably due to 2-pentanol. Further investigations are ongoing.

All nanomaterials were used in the hydrogenation of o-methylanisole (Scheme 1), and the results (Table 1) revealed

Scheme 1. o-Methylanisole Hydrogenation
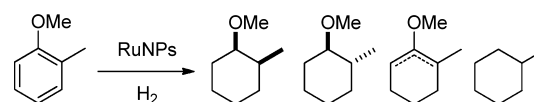
the crucial importance of the nature of the substituents on the phosphine for the catalytic activity. Materials containing only Ar$_3$P showed no or very poor activity (entries 3 and 5), and materials mainly containing Alk$_2$ArP (entries 1, 4 and 8) rendered complete hydrogenation of o-methylanisole. Comparison of entries 7 and 8 shows that full hydrogenation of the ligands to Alk$_3$P yielded slower catalysts than the partially hydrogenated ligands.

To demonstrate the ligand effect and the importance of Alk_2ArP as the ligand, $Ru5^{0.1}$ was prepared using directly ligand **5** containing cyclohexyl groups. The particles obtained are very similar in size (1.78 nm) to the ones obtained using **2** and the solubility is the same, and its ^1H and ^{31}P HRMAS NMR spectra are almost identical to those of $Ru2^{0.2}$ (see SI, Figures S7 and S8). The conversion provided by $Ru5^{0.1}$ in o-methylanisole hydrogenation was lower than that of the most active materials, but still much higher than that of $Ru2^{0.1}$, and moreover, it gave the best selectivity (>30%) toward partial hydrogenation, with no additives necessary.

Kinetic studies were carried out with the three most active catalysts ($Ru4^{0.2}$, $Ru1^{0.1}$, and $Ru2^{0.2}$), one of medium activity ($Ru3^{0.2}$) and the one prepared with Cy_2P ligand **5** ($Ru5^{0.1}$) (Figure 5). As can be seen, $Ru4^{0.2}$ is the most active material,
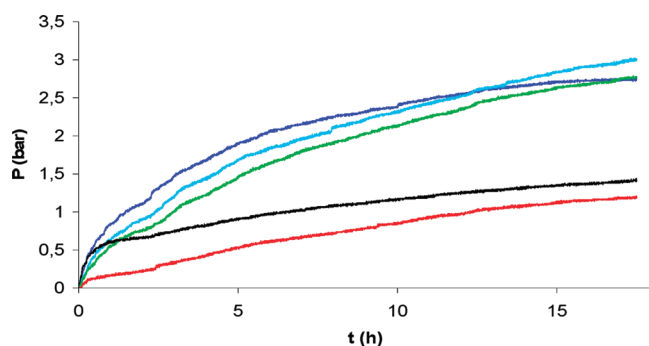

Figure 5. Monitoring of o-methylanisole hydrogenation. Reaction conditions: 40 bar, 295 K, 0.125 M in THF and 0.33% of total Ru. Dark blue: $Ru4^{0.2}$. Light blue: $Ru1^{0.1}$. Green: $Ru2^{0.2}$. Red: $Ru3^{0.2}$. Black: $Ru5^{0.1}$.

followed by $Ru1^{0.1}$ and $Ru2^{0.2}$, respectively; these activities correspond directly to the proportion of Alk_2ArP observed in the ^{31}P HRMAS NMR spectra. The kinetic study also revealed that the initial activity of $Ru5^{0.1}$ is even higher than that of $Ru4^{0.2}$, but its activity decreases markedly after a half hour, which could be due to a complete hydrogenation of **5** under reaction conditions and, thus, the destabilization of the NPs.

Aryls can interact with the surface of the NPs, but alkyls usually do not. This may explain why triarylphosphine-RuNPs are inactive (their aryls are over the faces of the nanoparticles, thus blocking the access of the substrate to the active site) but Cy_2PAr-RuNPs show high activities. The higher activity of $Ru4^{0.2}$ is probably due to the fact that hydrogenated monophosphine **4** can give faster access of the substrate to the active site (faces occupied by the aromatic backbone) than the diphosphines as a result of its flexibility. In addition, an electronic effect may be involved because Alk_2ArP are stronger donor ligands than Ar_3P, and thus, the former produces electronically richer NPs.

One might say that ligand hydrogenation takes place on RuNPs that happen to be active, and subsequently, these particles are also the ones that will hydrogenate anisole. The facts that fully hydrogenated ligands render catalysts of low activity and that "prehydrogenated" **5** gives also very active species prove that the activity is not an artifact of the RuNP synthesis but a ligand effect, with Cy_2PAr ligands giving the most active species.

It is also remarkable that no product derived from hydrogenolysis of the C−O bond was observed, although this is a common side reaction.[4,23,24] Perhaps this is related to a

reduced acidity of surface H species. This is curious moreover because C−O cleavage of THF does occur during the synthesis.

The most active material, $Ru4^{0.2}$, was also tested in benzene hydrogenation and provided one of the highest activities reported under mild conditions (TOF > 5000 h^{-1} at 3 bar and 295 K) and with TOF > 60,000 h^{-1} under standard conditions (40 bar, 393 K, solvent-free).

CONCLUSIONS

In summary, we have successfully used newly designed phosphine ligands especially optimized for NP stabilization and modification of the catalytic properties of RuNPs in arene hydrogenation. Moreover, we have shown that HRMAS NMR spectroscopy is a powerful tool for the characterization of phosphines directly attached to the RuNP surface and that their nature is directly related to the activity of the hydrogenation catalysts.

ASSOCIATED CONTENT

Ⓢ Supporting Information

Synthetic procedure, elemental analysis, NMR procedures and additional ^1H, ^{31}P and ^1H−^{31}P-HSQC HRMAS NMR spectra and 2D-DOSY experiments. This material is available free of charge via the Internet at http://pubs.acs.org.

AUTHOR INFORMATION

Corresponding Author
*E-mail: pvanleeuwen@iciq.es.

Notes
The authors declare no competing financial interest.

ACKNOWLEDGMENTS

REFERENCES

(1) Schmid, G. *Nanoparticles, from Theory to Application*; Wiley-VCH: Weinheim, 2004.

(2) Huang, J.; Jiang, T.; Han, B. X.; Wu, W. Z.; Liu, Z. M.; Xie, Z. L.; Zhang, J. L. *Catal. Lett.* **2005**, *103*, 59−62.

(3) Zahmakiran, M.; Tonbul, Y.; Özkar, S. *J. Am. Chem. Soc.* **2010**, *132*, 6541.

(4) Gual, A.; Godard, C.; Castillón, S.; Claver, C. *Dalton Trans.* **2010**, *39*, 11499.

(5) Silveira, E. T; Umpierre, A. P.; Rossi, L. M.; Machado, G.; Morais, J.; Soares, G. V.; Baumvol, I. J. R.; Teixeira, S. R.; Fichtner, P. F. P.; Dupont, J. *Chem.—Eur. J.* **2004**, *10*, 3734.

(6) Bu, J.; Liu, J.-L.; Chen, X.-Y.; Zhuang, J.-H.; Yan, S.-R.; Qiao, M.-H.; He, H.-Y.; Fan, K.-N. *Catal. Comm.* **2008**, *9*, 2612.

(7) Schwab, F.; Lucas, M.; Claus, P. *Angew. Chem. Int. Ed.*. **2011**, *50*, 10453.

(8) López-Valbuena, J. M.; Escudero-Adán, E. C.; Benet-Buchholz, J.; Freixa, Z.; van Leeuwen, P. W. N. M. *Dalton Trans.* **2010**, *39*, 8560.

(9) Tschan, M. J. L.; López-Valbuena, J. M.; Freixa, Z.; Launay, H.; Hagen, H.; Benet-Buchholz, J.; Leeuwen, P. W. N. M. *Organometallics* **2011**, *30*, 792.

(10) Posset, T.; Blumel, J. *J. Am. Chem. Soc.* **2006**, *128*, 8394.

(11) Polito, L.; Colombo, M.; Monti, D.; Melato, S.; Caneva, E.; Prosperi, D. *J. Am. Chem. Soc.* **2008**, *130*, 12712.

(12) Zhou, H. Y.; Du, F. F.; Li, X.; Zhang, B.; Li, W.; Yan, B. *J. Phys. Chem. C* **2008**, *112*, 19360.

(13) Espinosa, J. F. *Curr. Top. Med. Chem.* **2011**, *11*, 74.

(14) Pan, C.; Pelzer, K.; Philippot, K.; Chaudret, B.; Dassenoy, F.; Lecante, P.; Casanove, M. J. *J. Am. Chem. Soc.* **2001**, *123*, 7584.

(15) Philippot, K.; Chaudret, B. *Oil Gas Sci. Technol. Rev. IFP* **2007**, *62*, 799.

(16) García-Antón, J.; Axet, M. R.; Jansat, S.; Philippot, K.; Chaudret, B.; Pery, T.; Buntkowsky, G.; Limbach, H. H. *Angew. Chem., Int. Ed.* **2008**, *47*, 2074.

(17) In Ru4$^{0.2}$, the backbone aromatic ring without the phosphino group is also reduced.

(18) Lara, P.; Rivada-Wheelaghan, O.; Conejero, S.; Poteau, R.; Philippot, K.; Chaudret, B. *Angew. Chem., Int. Ed.* **2011**, *50*; DOI 10.1002/anie.201106348.

(19) Diéguez, M.; Pàmies, O.; Mata, Y.; Teuma, E.; Gómez, M.; Ribaudo, F.; van Leeuwen, P. W. N. M. *Adv. Synth. Catal.* **2008**, *350*, 2583.

(20) Favier, I.; Massou, S.; Teuma, E.; Philippot, K.; Chaudret, B.; Gómez, M. *Chem. Commun.* **2008**, 3296.

(21) Escárcega-Bobadilla, M. V.; Tortosa, C.; Teuma, E.; Pradel, C.; Orejón, A.; Gómez, M.; Masdeu-Bultó, A. M. *Catal. Today* **2009**, *148*, 398.

(22) Somorjai, G. A.; Frei, H.; Park, J. Y. *J. Am. Chem. Soc.* **2009**, *131*, 16589.

(23) Widegren, J. A.; Finke, R. G. *Inorg. Chem.* **2002**, *41*, 1558.

(24) Fonseca, G. S.; Umpierre, A. P.; Fichtner, P. F. P.; Teixeira, S. R.; Dupont, J. *Chem.—Eur. J.* **2003**, *9*, 3263.